

Ground state of the quantum anisotropic planar rotor model: A finite size scaling study of the orientational order–disorder phase transition

Balázs Hetényi^{a)}

Department of Chemistry, Columbia University, 3000 Broadway, New York, New York 10027
and Department of Chemistry, Princeton University, Princeton, New Jersey 08544

Bruce J. Berne

Department of Chemistry, Columbia University, 3000 Broadway, New York, New York 10027

(Received 5 September 2000; accepted 10 November 2000)

The ground state properties of the quantum anisotropic planar rotor (QAPR) model, which was constructed to describe the orientational ordering of homonuclear diatomic molecules on inert surfaces, are investigated theoretically using diffusion Monte Carlo. The implementation of the descendant weighing (DW) technique due to Casulleras and Boronat [Phys. Rev. B **52**, 3654 (1995)] is used, for which an alternate derivation is presented, based on the path-integral representation of the imaginary time propagator. We calculate the order parameter and then perform finite size scaling in order to search for a critical reduced rotational constant B_c^* at zero temperature. Our simulation results indicate that a critical rotational constant is at $B_c^* \approx 0.25$. The behavior of the kinetic and potential energies show strong evidence for local, single-rotor tunneling as the driving mechanism for the phase transition. A Gaussian mean-field treatment is also presented, in which the most important mechanism is local, single-rotor tunneling. While quantitatively the mean-field phase transition is not in agreement with the simulation results, the energy curves show qualitative similarities. In both cases, the phase transition occurs at the point where the kinetic energy reaches a maximum as a function of the reduced rotational constant B^* . © 2001 American Institute of Physics. [DOI: 10.1063/1.1337858]

I. INTRODUCTION

The anisotropic planar rotor (APR) model^{1–3} and its quantum generalization (QAPR) (Ref. 4) are minimalist models that were constructed to describe the orientational ordering of homonuclear diatomic molecules on inert surfaces. For an extensive review on the subject of homonuclear diatomic molecules physisorbed on inert surfaces, see Ref. 3. According to the assumptions of the model, the centers of mass of the molecules are fixed on a two-dimensional lattice. The molecules have fixed bondlengths and they perform uniaxial rotation. They interact via the anisotropic part of the electrostatic quadrupolar potential, and only nearest neighbor interactions are taken into account.

A system that can be modeled by the APR model and one that has received attention experimentally is N₂ physisorbed on graphite. It has been shown that at coverages less than 1/3 the number of hexagons of the graphite surface and at temperatures $T < 47$ K the molecules are translationally ordered and their centers of mass form an equilateral triangular lattice.^{5,6} If the system is cooled below 30 K, the system undergoes an orientational phase transition.^{7–11} It has been shown both experimentally⁹ and theoretically (using the APR model)² that the low temperature orientationally ordered phase is of the “herringbone” structure.

The order of the phase transition has been suspected to be “weakly” first order experimentally.^{9,10} Theoretically the

order of the phase transition in the APR model has been a controversial issue. An investigation based on a large scale simulation of the classical system¹² concluded that the transition is “weakly” first order. Our more recent study¹³ of the QAPR model concluded that the phase transition is continuous. This conclusion was based on the calculation of cumulants^{14–16} which have a universal value at the phase transition point that is known in the case of a first order phase transition.¹⁷

Investigations of the phase diagram of the QAPR model^{4,18,19} have given rise to an interesting question regarding the possibility of a *re-entrant* phase transition. In a re-entrant phase transition the system goes from an ordered state into a disordered state upon lowering of the temperature. The Hamiltonian of the QAPR model has two parameters: the rotational constant B and the coupling constant J . One can set the energy scale to be either one of those parameters, and thus analyze the system in terms of a one parameter Hamiltonian. Marx and Nielaba⁴ have analyzed the reduced rotational constant (B^*) vs reduced temperature (T^*) phase diagram and they have predicted that there is a range of rotational constants ($0.4 < B^* < 0.7$) where upon cooling, the system first enters an ordered phase, and subsequently reenters the disordered phase. The investigation of Martoňák *et al.* found a reentrant phase transition in the mean field analysis of the model, but this result was not supported by their simulations. Based on a zero temperature study Müser and Ankerhold²⁰ found a phase transition point at $B_c^* \approx 0.4$, which in conjunction with the finite temperature results of

^{a)}Present address: Department of Chemistry, Princeton University, Princeton, New Jersey 08544.

the earlier studies cited here is evidence for re-entrance.

Direct evidence for the existence of reentrance in the QAPR model was presented by Hetényi *et al.*¹³ In this study, the order parameter and its moments were calculated by path-integral Monte Carlo (PIMC),^{21–24} and finite size scaling was performed to identify phase transition points.

In the finite temperature studies cited above, the PIMC algorithm was modified to account for the fact that the system is a set of one-dimensional rotors. In Ref. 13 an efficient sampling algorithm developed by Cao²⁵ was used.

At a reduced rotational constant of $B^* = 0.6364$ two phase transition points were found at reduced temperatures $T^* \approx 0.09$ and $T^* \approx 0.3$. At reduced temperatures $0.09 \leq T^* \leq 0.3$ the system was found to be in the ordered state. Investigation of the energies indicated that the low temperature reentrant phase transition is most likely caused by barrier penetration unique to quantum systems (tunneling).

It is important to note that reentrance has been found in two other systems. By Raman spectroscopy it has been shown that solid HD undergoes a pressure induced re-entrant orientational phase transition.²⁶ A reentrant phase transition has also been found experimentally^{27,28} in granular superconductors.²⁹ Theoretical investigations based on mean field^{30,31} and renormalization group theory,³² and simulations³³ have also resulted in a re-entrant phase diagram. The model used in the study of granular superconductors is the quantum generalization of the XY model. Both the QAPR and the quantum XY model consist of coupled one-dimensional rotors.

Previous ground state simulations²⁰ on the QAPR model did not include explicit investigation of the order parameter because ground state observables for quantum many-body systems are in general difficult to calculate. Although energies may be obtained from the diffusion Monte Carlo^{34–36} (DMC) method quite accurately, methods for extracting observables such as the descendant weighing technique³⁷ (DW) or the method of auxiliary fields^{38,39} have been plagued by difficulties in obtaining good statistics in the case of large systems. An alternative method in calculating ground state observables is the recently developed reptation quantum Monte Carlo algorithm.⁴⁰

The purpose of this paper is to investigate the orientational ordering behavior of the QAPR model at zero temperature. We perform a variational mean-field treatment using Gaussian basis functions and we study the system by DMC. In the DMC study, we calculate the order parameter directly and use finite size scaling in order to detect a transition point. We use an implementation of the descendant weighing (DW) technique due to Casulleras and Boronat⁴¹ that is more efficient than the standard implementation, and has been tested on systems with a large number of degrees of freedom. In this paper we give an alternate derivation of that particular implementation of DW described in Ref. 41. Our derivation is based on writing the imaginary time propagator in the path-integral representation.²⁴

The issues that arise in simulating one-dimensional rotations at low temperatures have been investigated elsewhere.^{42,43} Relying on the result presented in Ref. 43, we argue that the standard DMC algorithm is applicable to sys-

tems involving one-dimensional rotors in the calculation of observables which are of the same periodicity as the Hamiltonian of the system (this condition usually holds for physically relevant observables).

The paper is organized as follows. In the next section we describe the QAPR model and give the expression for the herringbone order parameter. In Sec. III we review the DMC method and address its application to systems involving one-dimensional rotors. We also present a derivation and implementation of DW as applied in Ref. 41. In Sec. IV we briefly present the expressions for the cumulants we use to perform finite size scaling. In Sec. V we present our Gaussian mean-field treatment. In Sec. VI we present the simulation details. In Sec. VII we state the results of our DMC simulation, and in Sec. VIII we present our conclusions.

II. THE QAPR MODEL AND THE HERRINGBONE ORDER PARAMETER

The APR and QAPR models are minimalist models that have been shown to capture the main features of the results of experiments dealing with N₂ physisorbed on inert surfaces. The fundamental assumptions of the model are that the diatomics are fixed on a lattice (in our case triangular), they have fixed bond lengths, they perform uniaxial rotation, and they are coupled via the anisotropic part of the quadrupolar term of the multipole expansion of the potential. The full electrostatic quadrupole–quadrupole interaction includes an isotropic term as well, whose magnitude is less than one tenth that of the anisotropic term. For this reason only the anisotropic term was retained, and the isotropic term was neglected. These assumptions give rise to the QAPR Hamiltonian,

$$H = -B \sum_{i=1}^N \frac{\partial^2}{\partial \phi_i^2} + J \sum_{\langle i,j \rangle} \cos(2\phi_i + 2\phi_j - 4\theta_{ij}), \quad (1)$$

where N denotes the number of rotors, ϕ_i denotes the coordinate of rotor i , B and J denote the rotational and the anisotropic quadrupolar coupling constant, respectively. The summation in the second term is over nearest neighbors. The angles θ_{ij} have the value of the line connecting the molecules of a given bond. For a triangular lattice they are given by $\theta_{ij} = 0, \pi/3, 2\pi/3, \pi, 4\pi/3, 5\pi/3$. The APR model, which is the classical version of the QAPR model is obtained by writing the classical expression for the kinetic energy instead of the quantum expression in Eq. (1). In this study we use the reduced one parameter Hamiltonian obtained by setting $J = 1$.

The order parameter that is sensitive to herringbone ordering is a three component vector whose components ($\alpha = 1, 2, 3$) are given by

$$\Phi_\alpha = \frac{1}{N} \sum_{j=1}^N \sin(2\phi_j - 2\eta_\alpha) \exp[i\mathbf{Q}_\alpha \cdot \mathbf{R}_j], \quad (2)$$

where

$$\begin{aligned} \mathbf{Q}_1 &= \pi(0, 2/\sqrt{3}) \quad \eta_1 = 0, \\ \mathbf{Q}_2 &= \pi(-1, -1/\sqrt{3}) \quad \eta_2 = 2\pi/3, \\ \mathbf{Q}_3 &= \pi(1, -1/\sqrt{3}) \quad \eta_3 = 4\pi/3, \end{aligned} \quad (3)$$

and \mathbf{R}_i denote the lattice points on the triangular lattice. In this study we will evaluate the magnitude of the three component vector in Eq. (2) and its moments.

III. THE DIFFUSION MONTE CARLO METHOD AND CALCULATION OF OBSERVABLES

A. The diffusion Monte Carlo method

In this section we give a brief description of DMC. For more elaborate descriptions we refer the reader to the original work of Anderson^{34–36} or a more recent review.⁴⁴

The time-dependent Schrödinger equation in imaginary time for an arbitrary system with Hamiltonian H is written as

$$\begin{aligned} \frac{\partial \Psi(x, \tau)}{\partial \tau} &= -H\Psi(x, \tau) \\ &= \frac{1}{2m} \frac{\partial^2}{\partial x^2} \Psi(x, \tau) - V(x)\Psi(x, \tau), \end{aligned} \quad (4)$$

where x denotes the coordinate of the system, $V(x)$ denotes the potential energy. We have used atomic units. For notational simplicity, we use a one-dimensional system, but the concepts are trivially generalizable to the many-dimensional case. The formal solution of Eq. (4) may be written

$$\Psi(x, \tau) = \sum_i c_i \phi_i(x) \exp(-E_i \tau), \quad (5)$$

where $\phi_i(x)$ and E_i are the eigenfunctions and eigenvalues of the time-independent Schrödinger equation,

$$H\phi_i(x) = E_i \phi_i(x). \quad (6)$$

We may shift the energy of the system by a reference value E_R and rewrite Eq. (5) as

$$\Psi(x, \tau) = \sum_i c_i \phi_i(x) \exp[-(E_i - E_R)\tau]. \quad (7)$$

Note that the contributions of states whose energy E_i is less (more) than E_R will increase (decrease) exponentially. If E_R is chosen to be the ground state energy, then in the limit of long imaginary time, contributions from states other than the ground state will vanish exponentially, and the remaining contribution, which is from the ground state will be independent of imaginary time. The criterion for long imaginary time is

$$\tau \gg \frac{1}{E_1 - E_0}. \quad (8)$$

Finding the value of E_R that stabilizes the distribution of an imaginary time propagation is tantamount to determining the ground state energy.

In DMC a distribution is propagated according to Eq. (7). The distribution is represented by a set of replicas of the system. In a DMC short time step, each replica is given a random Gaussian displacement according to

$(2\pi\epsilon/m)^{1/2} \exp\{-m[x(\epsilon) - x(0)]^2/2\epsilon\}$ (where ϵ is the time of propagation), and then it is replicated or eliminated according to the probability $\exp[-(V(x) - E_R)\epsilon]$.

We note that in the DMC method a trial function may be used to improve sampling. Implementation of trial functions are described elsewhere.^{45,46}

Since the Hamiltonian of our system involves one-dimensional rotors, it is appropriate to address the question of winding numbers. Winding numbers arise in the path-integral representation of the partition function of systems with one-dimensional rotors. For a more detailed explanation of the winding number and its significance, see Refs. 47 and 48. At finite temperature care must be taken in incorporating the winding number into the simulation. Several approaches have been put forth in attaining this goal.^{49,25} In the case of zero temperature simulations one of the authors has recently proved⁴³ that the effect of the winding number can be neglected in the calculation of observables that have the periodicity of the system. Since all the observables we calculate obey this condition, we can use the DMC algorithm as described above to simulate the QAPR model.

B. Calculation of observables

The normalization constant which plays the role of the partition function at zero temperature can be written as

$$Q_{T=0} = \langle \Psi_g | \Psi_g \rangle = \int dx \Psi_g^2(x), \quad (9)$$

where Ψ_g is the ground state wave function. Ground state observables may be evaluated by averaging over the distribution $\Psi_g^2(x)$.

Using the Dirac notation we write the propagation of an arbitrary wave function in imaginary time as

$$|\Psi(\tau)\rangle = \exp(-\tau H) |\Psi(0)\rangle. \quad (10)$$

In the following derivation we assume that the wave functions are real. Let τ_c denote a duration in imaginary time that is large enough for excited states to have decayed. If the propagation time $\tau \gg \tau_c$ then $\Psi(\tau)$ will have negligible contributions from states other than the ground state. Since the wave function Ψ is arbitrary, we can take two arbitrary functions Ψ_1 and Ψ_2 , propagate them to two different imaginary times τ_1 and τ_2 . Provided that $\tau_1, \tau_2 \gg \tau_c$ we can obtain two good approximations to the ground state wave function,

$$|\Psi_g\rangle \approx \exp(-\tau_1 H) |\Psi_1\rangle \quad (11)$$

and

$$|\Psi_g\rangle \approx \exp(-\tau_2 H) |\Psi_2\rangle. \quad (12)$$

Using Eqs. (11) and (12), we may write an approximate expression for the normalization constant Eq. (9) as

$$Q_{T=0} = \int dx \langle \Psi_1 | \exp(-\tau_1 H) | x \rangle \langle x | \exp(-\tau_2 H) | \Psi_2 \rangle. \quad (13)$$

Inserting two coordinate identities, Eq. (13) becomes

$$Q_{T=0} = \int dx dx' dx'' \langle \Psi_1 | x' \rangle \langle x' | \exp(-\tau_1 H) | x \rangle \times \langle x | \exp(-\tau_2 H) | x'' \rangle \langle x'' | \Psi_2 \rangle. \quad (14)$$

Defining $\tau_t = \tau_1 + \tau_2$, Eq. (14) can be rewritten in the path-integral formulation as

$$Q_{T=0} = \int dx dx' dx'' \Psi_1(x') \Psi_2(x'') \times \int_{x(0)=x'}^{x(\tau_1)=x} \mathcal{D}[x(\tau')] \exp\left[-\int_0^{\tau_1} d\tau' H(\tau')\right] \times \int_{x'(\tau_1)=x}^{x'(\tau_t)=x''} \mathcal{D}[x'(\tau'')] \exp\left[-\int_{\tau_1}^{\tau_t} d\tau'' H(\tau'')\right]. \quad (15)$$

Equation (15) can be interpreted as follows. An arbitrary wave function Ψ_1 is propagated in imaginary time to τ_t and the resulting wave function is projected onto another arbitrary function Ψ_2 . At an intermediate time τ_1 such that $\tau_1 \geq \tau_c$ and $\tau_1 \leq \tau_t - \tau_c$ the coordinate x along the contributing paths is distributed according to a distribution that is a good approximation to $\Psi_g^2(x)$. Therefore, in principle it is possible to evaluate ground state observables by propagating an arbitrary function to imaginary time $\tau \geq 2\tau_c$ and averaging the values of the observables along those portions of the paths that are at imaginary times τ' , where $\tau_c \leq \tau' \leq \tau - \tau_c$.

As we have discussed above, DMC is a method that is capable of propagating distributions in imaginary time. The representatives of the distribution are replicas of the system (psips) which perform diffusive moves in space and then replicate or annihilate themselves according to the potential energy part of the imaginary time propagator. The psips trace out paths which terminate when a psip is annihilated. If a psip is annihilated at imaginary time τ_a then its ascendants between $\tau=0$ and $\tau=\tau_a$ trace out a path that can be viewed as a contributing path in the propagation of some arbitrary distribution from imaginary time $\tau=0$ to $\tau=\tau_a$. Alternatively, it can also be viewed as a contributing path of the propagation of an arbitrary distribution from imaginary time $\tau=\tau_a$ to $\tau=0$.

We can use DMC to sample the paths contributing to the propagation in Eq. (15). Consider the psips that arrive at the final time τ_t . Their ascendants trace out paths that contribute to a propagation of duration τ_t . Since the wave functions Ψ_1 and Ψ_2 are arbitrary, these paths can be viewed as the contributing paths in the path-integral expression of Eq. (15). Therefore coordinate dependent observables can be calculated by using the positions of the ascendants between imaginary times τ_c and $\tau_t - \tau_c$. Due to the fact that in the case of a DMC simulation Ψ_2 is the ground state wave function, ascendants after imaginary time τ_c can all be averaged.

The scheme presented above is equivalent to that put forth by Casulleras and Boronat.⁴¹ In their work it is viewed as an alternative implementation of DW. The implementation presented here and in Ref. 41 is considerably easier to program than the standard implementation of DW. After

imaginary time τ_c the averaging is started. For each psip the average is stored in an array whose leading dimension is equal to the instantaneous number of psips. When a psip is annihilated at some later imaginary time, the average for that psip is discarded. When a psip gives birth, its average is replicated. This way of sorting is exactly the same as the sorting of the coordinates after each time step.

IV. FINITE SIZE SCALING

Phase transitions occur in the thermodynamic limit. The sizes of systems that can be studied in the laboratory can essentially be regarded as being in the thermodynamic limit. In a computer simulation, however, the systems that are simulated are of sizes which are generally small compared to the sizes of systems that can be studied in laboratory experiments. In these finite systems the phase transition point is rounded and shifted compared to the phase transition point in the thermodynamic limit. Care must be taken in determining the exact phase transition point.

In the case of second-order phase transitions a scheme that allows for the determination of phase transition points has been constructed. Based on the finite size scaling hypothesis^{50,51} one can calculate ratios of the different moments of the order parameter (known as Binder cumulants¹⁴⁻¹⁶) which allow for the determination of the critical point. For a complete account of the application of the finite size scaling hypothesis, see Refs. 14-16. In the following we only review the properties of the cumulants which are essential in locating critical points.

The ratios of moments used in this study are the second and fourth order Binder cumulants, which are of the form

$$U_2(N) = 1 - \frac{\langle \Phi^2 \rangle}{3\langle \Phi \rangle^2}, \quad (16)$$

$$U_4(N) = 1 - \frac{\langle \Phi^4 \rangle}{3\langle \Phi^2 \rangle^2},$$

where N denotes the system size. As a result of the finite size scaling hypothesis, the Binder cumulants are size independent at a critical point. Using assumed forms of the distribution, Binder has shown¹⁴⁻¹⁶ that the cumulants approach trivial limiting values in the case of complete order or disorder. In the ordered state both $U_2(N)$ and $U_4(N)$ take the limiting value of 2/3, whereas in the disordered state both take the value of 0.

Calculating the cumulant as a function of rotational constant for different system sizes allows for the determination of the phase transition point. The value of the cumulant will be closer to the limiting value in both the ordered and the disordered state, the larger the system size, since the larger system is closer to the thermodynamic limit. At the critical point the cumulants are size independent. For this reason, identifying the crossing point is tantamount to locating the critical rotational constant.

V. VARIATIONAL MEAN-FIELD THEORY USING A GAUSSIAN TRIAL FUNCTION

In the work of Müser and Ankerhold²⁰ simple analytical models were used to corroborate the results of the simulation. A mean-field treatment of the QAPR Hamiltonian using a function that was a product of a linear combination of Gaussian functions resulted in an ordered ground state for all values of the reduced rotational constant.

In this section we perform a variational treatment similar to the one in Ref. 20. Our trial function is a product of *single* Gaussian functions. The advantage of using single Gaussian functions is that the only essential mechanism that affects the behavior of the model is local tunneling (i.e., penetration of barriers in the vicinity of local minima). We find that local tunneling alone can drive an order–disorder phase transition. Although the value of the critical rotational constant found by our Gaussian mean-field treatment differs from that of the simulation results, the energy curves show essential qualitative similarities. In the case of Gaussian mean-field theory, it can be shown analytically that the phase transition occurs at a value of the rotational constant where the kinetic energy reaches a maximum. This conclusion is in agreement with our simulation results in Sec. VII (see Fig. 6).

We use a separable trial function of the form,

$$\Psi = \prod_{i=1}^N \Phi(\phi_i - \bar{\phi}_i),$$

$$\Phi(\phi) = \left(\frac{2\alpha}{\pi}\right)^{1/4} \exp(-\alpha\phi^2),$$
(17)

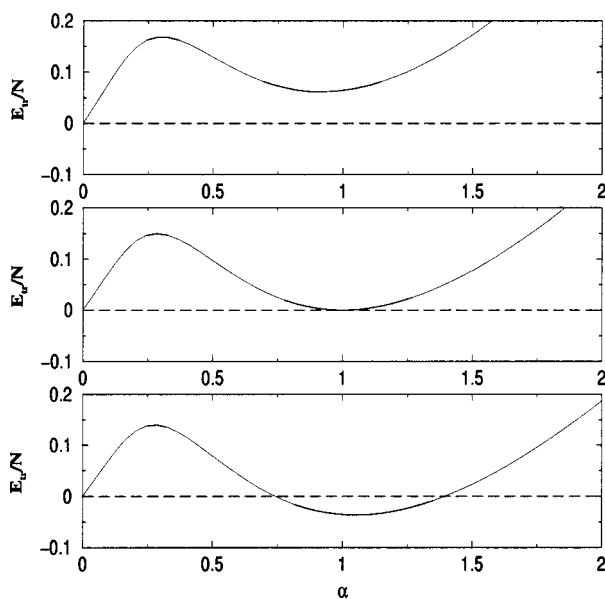


FIG. 1. Trial energy per particle E_{tr}/N as a function of the variational parameter α in the Gaussian mean-field approximation (lower panel $B^* = 0.7 < 2J^*/e$, middle panel $B^* = 2J^*/e$, upper panel $B^* = 0.8 > 2J^*/e$). For $B^* < 2J^*/e$ the minimum of the trial energy is lower than its value at $\alpha = 0$. For $B^* = 2J^*/e$ there are two minima, one at $\alpha = 0$, one at $\alpha = 1$. For $B^* > 2J^*/e$ the minimum is at $\alpha = 0$ and there is a local minimum at $\alpha > 0$. The presence of the two minima at $B^* = 2J^*/e$ indicate a first order phase transition at $B^* = 2J^*/e$.

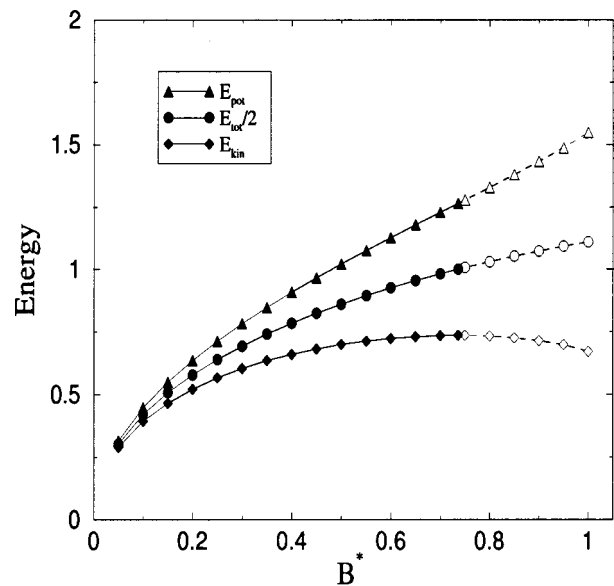


FIG. 2. Kinetic, potential, and half of the total energy as a function of reduced rotational constant in the Gaussian mean-field approximation. Filled symbols and solid lines indicate that the system is ordered ($B^* < 2J^*/e$). Unfilled symbols and dashed lines correspond to the trial function whose variational parameter α is obtained from the local minimum of the trial energy. In the ordered state, the kinetic energy increases as a function of the reduced rotational constant. It can be shown that at the critical point the derivative of the kinetic energy with respect to the reduced rotational constant B^* is zero. The potential energy increases throughout the range shown.

where $\bar{\phi}_i$ denotes the positions of the rotors in the herringbone structure (i.e., the classical minimum). Using the QAPR Hamiltonian [Eq. (1)] we obtain a trial energy of

$$E_{tr} = \langle \Psi | H | \Psi \rangle$$

$$= NB^* \alpha - 2N \exp(-1/\alpha).$$
(18)

Using the expression for the trial energy given in Eq. (18), it is an easy matter to show that a first order phase transition occurs at $B^* = 2/e$. Evidence for the critical rotational constant is provided in Fig. 1. For $B^* < 2/e$ the value of the minimization parameter α which minimizes the trial energy is some finite value $\alpha > 1$, corresponding to an ordered state. For $B^* > 2/e$ the value of the minimization parameter α which minimizes the trial energy is zero, which corresponds to a disordered state. Observables calculated based on the trial function of Eq. (17) change discontinuously as a function of B^* at $B^* = 2/e$.

In Fig. 2 we show the kinetic, potential, and half the total energy of the system in our Gaussian mean-field approximation. The potential energy is shifted by its value at the classical minimum ($V_c = 2$). The solid lines and filled symbols correspond to the system in its ordered state $B^* < 2/e$. The dashed line and opaque symbols correspond to results associated with the local minimum of the trial energy ($B^* > 2/e$).

The potential energy increases throughout the range of the reduced rotational constant shown. The kinetic energy increases until the phase transition point ($B_c^* = 2/e$). It is a trivial matter to show that the derivative of the kinetic energy with respect to B^* is zero at the phase transition point.

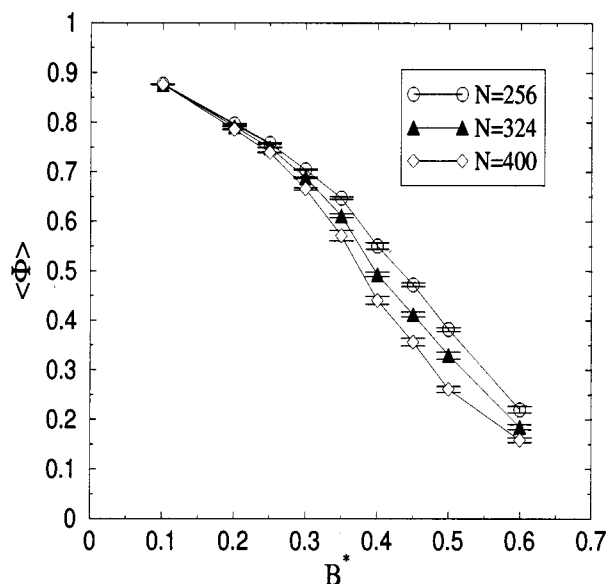


FIG. 3. Simulation results for the order parameter $\langle \Phi \rangle$ as a function of reduced rotational constant B^* for the QAPR model at zero temperature for system of size $N=256$, $N=324$, and $N=400$. The order parameter decreases steadily with increasing rotational constant for all three system sizes. The size dependence begins to increase at a reduced rotational constant of $B^* \approx 0.3$.

VI. SIMULATION DETAILS

We simulate QAPR systems of three different sizes ($N = 256, 324, 400$) by DMC. We use a trial function of the Jastrow form,

$$\Psi_J = \exp(-\gamma V), \quad (19)$$

where V denotes the potential energy function, and γ denotes a variational parameter. The variational parameter is obtained from a variational Monte Carlo simulation.

DMC simulations were run for 50 000 steps for relaxation, and 50 000 steps for observation. The time step of the run was $\Delta\tau = 0.01$. For the evaluation of the energy, the value of the reference energy was collected after every 10 time steps and averaged at the end. For other observables data was collected at every time step. Five different runs were made for each value of the reduced rotational constant B^* . The Binder cumulants presented were calculated by taking the averages of the five different runs.

VII. RESULTS

A. Order parameter and Binder cumulants

We calculated the order parameter defined as the magnitude of the three component vector defined in Eq. (2). The results are presented in Fig. 3. The order parameter decreases steadily as a function of rotational constant for all three system sizes. The size dependence increases beyond a reduced rotational constant of $B^* \approx 0.2$. The significant decrease in the order parameter and the fact that the size dependence of the order parameter varies is indicative of a phase transition.

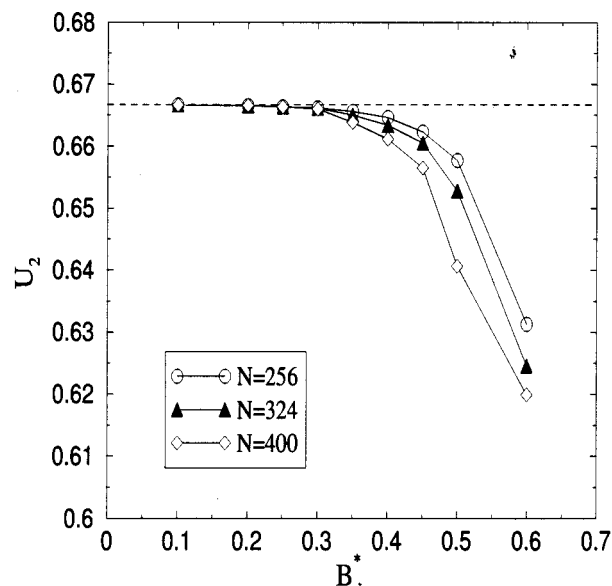


FIG. 4. Simulation results of the second order Binder cumulant U_2 as a function of reduced rotational constant B^* for systems of size $N=256$, $N=324$, and $N=400$. The dashed line is at a value of $2/3$. At low values of the reduced rotational constant ($B^* \leq 0.3$) the value of the cumulant approaches $2/3$ indicating an ordered state. At higher values ($B^* > 0.3$) the cumulant decreases significantly indicating a disordered state.

At reduced rotational constants of $B^* \leq 0.3$ the order parameter has a high value ($\langle \Phi \rangle \geq 0.65$), indicative of an ordered system.

In the interpretation of the behavior of the order parameter it is important to consider the competing effects that influence the ordering behavior of the system. In general a larger system is expected to behave more like an infinite system. This alone would mean that a system whose order parameter decreases with system size is disordered in the thermodynamic limit and vice versa. However the periodic boundary conditions, which tend to order the system, are more significant for small system sizes. It is most likely for this reason that the order parameter for the smallest system size has the largest value for almost all values of the reduced rotational constant that have been investigated (except $B^* = 0.1$).

We also calculated the second and fourth order Binder cumulants [U_2, U_4 respectively, see Eq. (16)] as a function of the reduced rotational constant B^* . The results are presented in Figs. 4 and 5. For low values of the reduced rotational constant ($B^* \leq 0.3$) the cumulants approach $2/3$ indicating an ordered state. For values $B^* > 0.3$ the cumulant decreases significantly indicating a disordered state. Also indicative of the disordered state is the fact that the cumulant of the large system has a lower value than the cumulant of the small system in the region $B^* > 0.3$. From the two graphs one can establish $B^* = 0.35$ as an approximate upper bound for the critical rotational constant.

While a definite crossing point is difficult to establish from the graphs, one can investigate the values of the Binder cumulants directly. In Table I we present the values of the fourth order Binder cumulants for reduced rotational con-

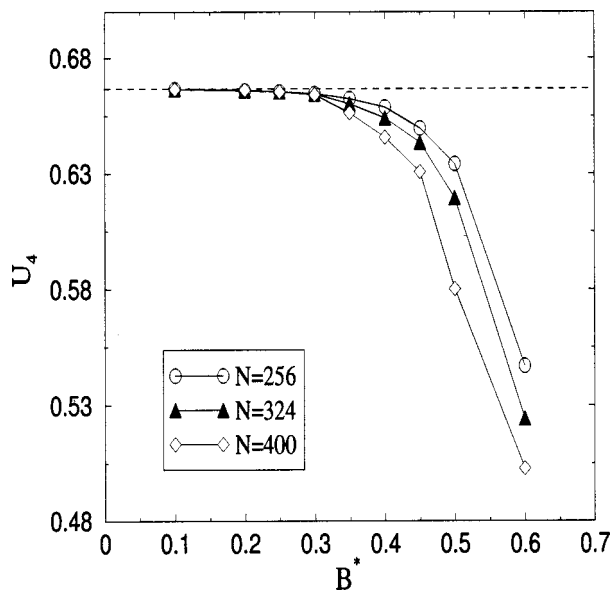


FIG. 5. Simulation results of the fourth order Binder cumulant U_4 as a function of reduced rotational constant B^* for systems of size $N=256$, $N=324$, and $N=400$. The dashed line is at a value of $2/3$. At low values of the reduced rotational constant ($B^* \leq 0.3$) the value of the cumulant approaches $2/3$ indicating an ordered state. At higher values ($B^* > 0.3$) the cumulant decreases significantly indicating a disordered state.

stants $B^* = 0.2, 0.25$, and 0.3 . The error bars shown are the standard deviation of the five runs.

The values of the fourth order Binder cumulant for $B^* = 0.2$ indicate that the system is ordered. For all three system sizes the fourth order Binder cumulant is close to $2/3$, moreover, the larger the system size the closer the value of the cumulant is to $2/3$. For $B^* = 0.3$ the trend as a function of system size reverses. For $B^* = 0.25$ the cumulants are approximately equal, and their error bars overlap. We conclude that the phase transition occurs at $B_c^* = 0.25$.

B. Energies

Investigating the energies has provided insight into the possible mechanism of the phase transition in previous studies (Refs. 13 and 20) of the QAPR model. In Ref. 13, the authors have argued, based on the behavior of the kinetic and potential energies, that the mechanism responsible for disordering the system at low temperatures is barrier penetration (tunneling).

TABLE I. Calculated values of the fourth order Binder cumulant U_4 as a function of several values of the reduced rotational constant B^* for systems of size $N=256$, $N=324$, and $N=400$. The number after \pm indicates the error in the last digit of the value of the cumulant. For the procedure used to estimate the error, see the text. For $B^* = 0.2$ ($B^* = 0.3$) the size dependence indicates that the system is ordered (disordered). A critical rotational constant is identified at $B_c^* = 0.25$.

B^*	$U_4(256)$	$U_4(324)$	$U_4(400)$
0.2	0.66594 ± 2	0.66603 ± 1	0.66610 ± 2
0.25	0.66534 ± 4	0.66538 ± 2	0.66539 ± 2
0.3	0.66463 ± 5	0.66449 ± 5	0.6641 ± 2

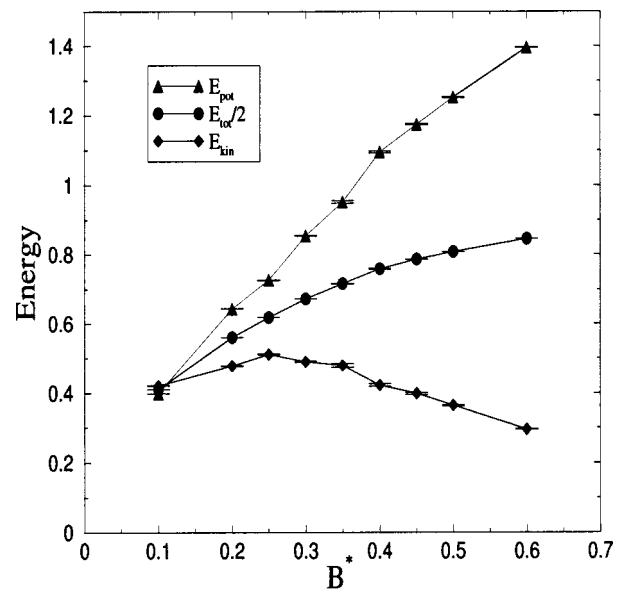


FIG. 6. Simulation results of half of the total ($E_{\text{tot}}/2$), kinetic (E_{kin}), and potential (E_{pot}) energies per particle as a function of the reduced rotational constant B^* for the $N=400$ system. Note that the potential energy is shifted by its value at the classical minimum ($E_{\text{min}}^{\text{cl}} = 2$). The values of the total energy and the potential energy show an increase with increasing reduced rotational constant throughout the range investigated. The value of the kinetic energy shows an initial increase, a plateau around the range of the critical rotational constant ($0.2 < B_c^* < 0.3$), and a subsequent decrease with increasing rotational constant.

In this study we have also calculated the potential, kinetic, and total energies. The total energy is calculated in the usual way,^{34–36} the potential energy is calculated by using the technique presented in Sec. III B. The kinetic energy is calculated indirectly by subtracting the potential energy from the total energy.

In Fig. 6 we present simulation results for the energies per rotor as a function of the reduced rotational constant (B^*) for the largest system ($N=400$). We show the kinetic, potential and half the total energies. The potential energy is shifted by the value of the classical minimum ($V_c = 2$), the average of the kinetic and potential energies and the kinetic energy.

The potential and total energies show an increase with increasing rotational constant for the range investigated. The kinetic energy, on the other hand, shows an initial increase, a maximum at the critical point ($B_c^* = 0.25$), and a subsequent decrease in the range $B^* > 0.25$. The “bulge” in the kinetic energy may be understood in terms of the relative importance of barrier penetration in the ordered and disordered phases. At low values of the reduced rotational constant ($B^* < 0.2$), both the kinetic and potential energies are low, indicating that the system is ordered (see also Fig. 3). In this region the system is behaving classically, tunneling does not seem to be significant. As the value of the reduced rotational constant is increased, the system begins to disorder ($0.2 < B^* < 0.3$). As the value of the reduced rotational constant increases further, the value of the kinetic energy decreases and the value of the potential energy increases. In this region the behavior of the system is dominated by quantum effects. The increase in potential energy corresponds to barrier pen-

etration by single rotors. The decrease in kinetic energy corresponds to imaginary velocities which can be associated with barrier penetration (tunneling) as well.

The above result and its interpretation is in strong qualitative agreement with our Gaussian mean-field analysis of Sec. V. In the Gaussian mean-field treatment the phase transition occurred precisely where the kinetic energy reached a maximum as a function of the reduced rotational constant. Furthermore since the trial function in our Gaussian mean-field study was such that only local barrier penetration was taken into account, the qualitative similarities between the behavior kinetic energies Gaussian model and the simulation indicate that the phase transition is driven by quantum tunneling.

Our simulation results are also in qualitative agreement with the results of Müser and Ankerhold.²⁰ In that study the dimensionless kinetic energy was calculated using the auxiliary field method.^{38,39} The dimensionless kinetic energy was found to increase in the region $0 < B^* < 0.4$. A change in the slope of the dimensionless kinetic energy was found at $B^* = 0.4$, beyond which the kinetic energy was found to decrease.

VIII. CONCLUSION

In this paper we have carried out a Gaussian mean-field treatment and a detailed numerical analysis of the ground state of the quantum anisotropic planar rotor (QAPR) model.

Our Gaussian mean-field treatment was based on a trial function which was a product of single Gaussians. Thus only single rotor tunneling was taken into account. A critical reduced rotational constant of $B_c^* = 2/e$ was found. Furthermore the phase transition in the mean-field model takes place exactly where the kinetic energy reaches a maximum as a function of the reduced rotational constant.

Our numerical studies consisted of diffusion Monte Carlo (DMC) simulations. We used an implementation of the descendant weighing (DW) technique which has been shown to provide results for systems with many degrees of freedom. We have studied the ordering of the system by way of finite size scaling of the order parameter. We have also calculated the total, potential, and kinetic energies of the system, in order to understand the mechanism behind the ordering behavior of the QAPR model at zero temperature.

The order parameter as a function of reduced rotational constant was shown to undergo a sizable decrease indicating a transition from an ordered state to a disordered state in the range of rotational constants investigated. Based on the values of the Binder cumulants the critical rotational constant was determined to be $B_c^* < 0.25$.

Investigation of the kinetic, potential, and total energies provided information about the importance of tunneling by single rotors in bringing about the order-disorder transition in the QAPR model. In the ordered phase ($B^* < 0.2$) both the kinetic and potential energies have relatively low values, indicating that the system is behaving classically. Barrier penetration in this range of rotational constants is negligible. In the transitional region ($0.2 < B^* < 0.3$) the potential was found to increase, but the kinetic energy was found to reach

a maximum. In the Gaussian mean-field model the phase transition was also accompanied by a maximum in the kinetic energy. For values of the reduced rotational constant ($B^* > 0.3$) (in the disordered phase) the potential energy was found to increase, however, the kinetic energy was found to decrease.

The behavior of the kinetic and potential energies was interpreted as a manifestation of tunneling. The potential energy increased due to barrier penetration by single rotors. The decrease in kinetic energy can also be associated with tunneling, since the kinetic energy is negative in regions in which the potential energy is higher than the total energy. In fact, according to our results, the transition from an ordered state to a disordered state at zero temperature in the QAPR model is brought about by single rotor tunneling.

ACKNOWLEDGMENTS

This work was supported by a grant to B.J.B. from the National Science Foundation. We would like to thank Dr. M. Pavese, Dr. M. H. Müser, Professor E. Šimánek, Professor Z. Rácz, Professor R. Martoňák, and Professor D. Marx for helpful discussions.

- ¹S. F. O'Shea and M. L. Klein, *Chem. Phys. Lett.* **66**, 381 (1979).
- ²O. G. Mouritsen and A. J. Berlinsky, *Phys. Rev. Lett.* **48**, 181 (1982).
- ³D. Marx and H. Wiechert, *Adv. Chem. Phys.* **95**, 213 (1996).
- ⁴D. Marx and P. Nielaba, *J. Chem. Phys.* **102**, 4538 (1995).
- ⁵J. K. Kjems, L. Passell, H. Taub, and J. G. Dash, *Phys. Rev. Lett.* **32**, 724 (1974).
- ⁶J. K. Kjems, L. Passell, H. Taub *et al.*, *Phys. Rev. B* **13**, 1446 (1976).
- ⁷T. T. Chung, *Surf. Sci.* **66**, 559 (1977).
- ⁸J. Eckert, W. D. Ellenson, J. B. Hastings, and L. Passell, *Phys. Rev. Lett.* **43**, 1329 (1979).
- ⁹R. D. Diehl, M. F. Toney, and S. C. Fain, Jr., *Phys. Rev. Lett.* **48**, 177 (1981).
- ¹⁰N. S. Sullivan and J. M. Vaissiere, *Phys. Rev. Lett.* **51**, 658 (1983).
- ¹¹A. D. Migone, H. K. Kim, M. H. W. Chan *et al.*, *Phys. Rev. Lett.* **51**, 192 (1983).
- ¹²O. Opitz, D. Marx, S. Sengupta *et al.*, *Surf. Sci. Lett.* **297**, L122 (1993).
- ¹³B. Hetényi, M. H. Müser, and B. J. Berne, *Phys. Rev. Lett.* **83**, 4606 (1999).
- ¹⁴K. Binder, *Annu. Rev. Phys. Chem.* **37**, 401 (1992).
- ¹⁵K. Binder, *Ferroelectrics* **73**, 43 (1987).
- ¹⁶K. Binder, *Phys. Rev. Lett.* **47**, 693 (1981).
- ¹⁷K. Vollmayr, J. D. Reger, M. Scheucher, and K. Binder, *Z. Phys. B: Condens. Matter* **91**, 113 (1993).
- ¹⁸R. Martoňák, D. Marx, and P. Nielaba, *Phys. Rev. E* **55**, 2184 (1997).
- ¹⁹D. Marx and P. Nielaba, *Phys. Rev. A* **45**, 8968 (1992).
- ²⁰M. H. Müser and J. Ankerhold, *Europhys. Lett.* **44**, 216 (1998).
- ²¹D. M. Ceperley, *Rev. Mod. Phys.* **67**, 279 (1995).
- ²²D. Chandler, in *Liquids, Freezing, and Glass Transition*, edited by D. Levesque, J. P. Hansen, and J. Zinn-Justin (North-Holland, Amsterdam, 1991), Chap. 4, pp. 193–285.
- ²³B. J. Berne and D. Thirumalai, *Annu. Rev. Phys. Chem.* **37**, 401 (1986).
- ²⁴R. P. Feynman and A. R. Hibbs, *Quantum Mechanics and Path Integrals* (McGraw-Hill, New York, 1965).
- ²⁵J. Cao, *Phys. Rev. E* **49**, 882 (1993).
- ²⁶F. Moshary, N. H. Chen, and I. F. Silvera, *Phys. Rev. Lett.* **71**, 3814 (1993).
- ²⁷S. Kobayashi, Y. Tada, and W. Sasaki, *J. Phys. Soc. Jpn.* **49**, 2075 (1980).
- ²⁸T. H. Lin, X. H. Shao, M. K. Wu *et al.*, *Phys. Rev. B* **29**, 1493 (1984).
- ²⁹E. Šimánek, *Inhomogeneous Superconductors: Granular and Quantum Effects* (Oxford University Press, Oxford, 1994).
- ³⁰E. Šimánek, *Phys. Rev. B* **32**, 500 (1985).
- ³¹M. V. Simkin, *Phys. Rev. B* **44**, 7074 (1991).
- ³²J. V. José, *Phys. Rev. B* **29**, 2836 (1984).

- ³³L. Jacobs, J. V. José, and M. A. Novotny, *Phys. Rev. Lett.* **53**, 2177 (1984).
- ³⁴J. B. Anderson, *J. Chem. Phys.* **73**, 3897 (1980).
- ³⁵J. B. Anderson, *J. Chem. Phys.* **65**, 4121 (1976).
- ³⁶J. B. Anderson, *J. Chem. Phys.* **63**, 1499 (1975).
- ³⁷K. E. Schmidt and M. H. Kalos, in *Applications of the Monte Carlo Method in Statistical Physics*, edited by K. Binder (Springer, Berlin, 1984).
- ³⁸R. D. Amos, *Adv. Chem. Phys.* **67**, 99 (1987).
- ³⁹P. Sandler, V. Buch, and D. C. Clary, *J. Chem. Phys.* **101**, 6353 (1994).
- ⁴⁰S. Baroni and S. Moroni, *Phys. Rev. Lett.* **82**, 4745 (1999).
- ⁴¹J. Casulleras and J. Boronat, *Phys. Rev. B* **52**, 3654 (1995).
- ⁴²P. Henelius, S. M. Girvin, and A. W. Sandvik, *Phys. Rev. B* **57**, 13382 (1998).
- ⁴³B. Hetényi, *Phys. Rev. E* **61**, 3220 (2000).
- ⁴⁴M. A. Suhm and R. O. Watts, *Phys. Rep.* **204**, 293 (1991).
- ⁴⁵D. M. Ceperley and B. J. Alder, *Phys. Rev. Lett.* **45**, 566 (1980).
- ⁴⁶D. M. Ceperley, *Phys. Rev. B* **18**, 3126 (1978).
- ⁴⁷W. K. Burton and A. H. De Borde, *Nuovo Cimento* **2**, 197 (1955).
- ⁴⁸L. S. Schulman, *Techniques and Applications of Path Integration* (Wiley-Interscience, New York, 1981).
- ⁴⁹D. Marx, S. Sengupta, and P. Nielaba, *J. Chem. Phys.* **99**, 6031 (1993).
- ⁵⁰V. Privman and M. E. Fisher, *Phys. Rev. B* **30**, 322 (1984).
- ⁵¹M. E. Fisher, *Phys. Rev. Lett.* **28**, 1516 (1972).